Sedimentary Geology 229 (2010) 144–159

Contents lists available at ScienceDirect

Sedimentary Geology

journal homepage: www.elsevier.com/locate/sedgeo

Hyperpycnal-fed turbidite lobe architecture and recent sedimentary processes: A case study from the Al Batha turbidite system, Oman margin

J. Bourget [a,*], S. Zaragosi [a], T. Mulder [a], J.-L. Schneider [a], T. Garlan [b], A. Van Toer [c], V. Mas [d], N. Ellouz-Zimmermann [e]

[a] Université Bordeaux I, UMR CNRS 5805 EPOC, Avenue des Facultés, F-33405 Talence, France
[b] SHOM, Centre Hydrographie, BP 426, F-29275 Brest, France
[c] LSCE/IPSL, CEA–CNRS–UVSQ, F-91198 Gif sur Yvette Cedex, France
[d] IFREMER, GM/LES, BP70, F-29280 Plouzané Cedex, France
[e] Institut Français du Pétrole (IFP), rue Bois Préau, F-92852 Rueil-Malmaison, France

ARTICLE INFO

Available online 5 April 2009

Keywords:
Turbidite system
Oman margin
Lobe
Hyperpycnite
Gravity flow
Arabian Sea

ABSTRACT

The main sediment depocenter along the Oman margin is the Al Batha turbidite system that develops in the Gulf of Oman basin. It is directly connected to the wadi Al Batha, and forms a typical sand and mud rich point source system that acts as regional sediment conduit and feeds a ~1000 km^2 sandy lobe.

The Al Batha lobe depositional architecture has been investigated in detail using very high-resolution seismic, multibeam echosounder data and sediment cores. Several scales of depositional architecture can be observed. The Al Batha lobe is composed of several depositional units, made of stacked elementary sediment bodies (thinner than 5 m) that are each related to a single flow event. The lobe is connected to the feeder system through a channel–lobe transition zone (CLTZ) that extends on more than 25 km. The lobe can be divided into proximal, middle and distal lobe areas. The proximal lobe is an area of erosion and by-pass with small axial feeder channels that rapidly splay into several small distributaries. They disappear in the mid-lobe area where deposits consist of vertically stacked tabular to lens-shaped sediment bodies, with a lateral continuity that can exceed 10 km. The distal lobe fringe shows a classical facies transition towards thin-bedded basin plain deposits.

Sub-surface deposits consist of sandy turbidites and hyperpycnites, interbedded with fine-grained deposits (thin turbidites, hyperpycnites, or hemipelagites). Although these distal deposits are mainly related to flow transformations and concentration evolution, they highlight the importance of flooding of the wadi Al Batha on the sediment transfer to the deep basin. The thick sandy hyperpycnites recovered in such a distal area are also possibly related to the initial properties of gravity flows, in relation to the flooding characteristics of mountainous desert streams.

Finally, the Al Batha lobe depositional architecture is typical of sand-rich lobes found within “small”, sand and mud rich turbidite systems fed by mountainous “dirty” rivers. Turbidite sedimentation in the Al Batha system appears to be primarily controlled by the strong climatic and geomorphic forcing parameters (i.e. semi-arid environment with ephemeral, mountainous rivers subjected to flash-flooding).

1. Introduction

Understanding the triggering mechanisms for submarine gravity flows is of primary importance because turbidite systems are made of different architectural elements directly related to the gravity flows properties (i.e. flow concentration, duration, sand/mud ratio, and flow transformation) which in turn depend on the changes in sea level and the type of margin setting (Piper and Normark, 2001).

Since the concept of hyperpycnal flows (Bates, 1953), the dynamics of flood-generated gravity currents and their influence on the growth of deep-sea turbidite systems have received considerable attention (e.g., Mulder and Syvitski, 1995; Mulder et al., 2001; Piper and Normark, 2001; Mulder et al., 2003; Mutti et al., 2003; among others). The importance of sediment delivery mechanisms in relation with the fluvial drainage basin is thus to be considered as a predominant control on deep-sea fans growth and architecture.

In submarine turbidite systems, sandy depositional lobes commonly accumulate at the termination of submarine feeder conduit, forming important hydrocarbon reservoirs. In ancient outcrops and on the modern sea floor, past studies have demonstrated that lobes show considerable architectural variability that may provide information about the gravity flows properties and their sediment source characteristics (Normark and Piper, 1991). Recent data from modern

* Corresponding author. Tel.: +33 540 008 381.
E-mail address: j.bourget@epoc.u-bordeaux1.fr (J. Bourget).

0037-0738/$ – see front matter © 2009 Elsevier B.V. All rights reserved.
doi:10.1016/j.sedgeo.2009.03.009

turbidite systems showed that lobes are not simply massive sheet-like deposits at the end of channel–levee systems, as previously thought, but are channelized and made of several *internal units* that are in turn composed by numerous *elementary sedimentary bodies* (Twichell et al., 1992; Piper et al., 1999; Savoye et al., 2000; Gervais et al., 2006b; Deptuck et al., 2008).

This paper focuses on the main sediment depocentre on the Oman passive margin (Gulf of Oman, NW Indian Ocean), the Al Batha turbidite system. Using multibeam echosounder data and high-resolution seismic profiles, we describe the internal architecture of the Al Batha lobe and its longitudinal organisation. The sedimentary deposits were also investigated from sediment cores to better understand depositional processes and flow initiation, and their relation to the specifics of the subaerial drainage basin. Finally, this study aims to provide a first description of the organisation of deep-sea sedimentation along this previously poorly explored margin.

2. Regional setting

2.1. Physiography

The Gulf of Oman is a triangular, 3400 m deep, 300 km wide and 950 km long semi-confined sedimentary basin (Fig. 1). It is located between the Oman passive margin and the Makran accretionary wedge (Iran and Pakistan margins), which developed in response to the northward subduction of the Arabian Sea beneath the Iranian and Afghan continental blocks since the Late Cretaceous (Byrne et al., 1992; Ellouz-Zimmermann et al., 2007). The basin is flanked on its eastern side by the 420 km long and 50 to 20 km wide northeast-trending Murray Ridge. The latter is considered to be a divergent plate boundary with low spreading rates (Gordon and Demets, 1989), and to be morphologically the northernmost extension of the Owen ridge and fracture zone, which corresponds to the Indian–Arabian plate boundary (Fournier et al., 2008) (Fig. 1).

2.2. Regional climate, drainage system and coastal hydrodynamics

The Arabian Sea is under the influence of the Asian monsoon-climate (Clemens and Prell, 2003). During summer months (June to September), winds blow from the south-west (e.g., SW-monsoon winds), and strongly affect the surface circulation of the Gulf of Oman. On land, due to the present day boreal summer position of the Intertropical Convergence Zone (ITCZ) along the southern coast of the Arabian Peninsula, only the southern Oman is directly affected by the moist monsoon air masses (Wheater and Bell, 1983; Fleitmann et al., 2007; Fuchs and Buerkert, 2008). Our study area lies further north, where arid to hyper-arid conditions dominate (Fuchs and Buerkert, 2008) and where precipitation occurs only episodically. Thus, rainfall in the area is very variable and can be extremely low or even absent for several years (Fuchs and Buerkert, 2008). During winter (November to March), cyclonic low-pressure systems originating in the eastern Mediterranean occasionally penetrate the Arabian landmass (Weyhenmeyer et al., 2000), and generate severe storms (Wheater and Bell, 1983; Fleitmann et al., 2007). Torrential rainfall can also occur during strong and hot summer monsoons, particularly during extreme events such as the Gonu cyclone (June 2007) that caused 6–8 days long flooding both in Oman and Iran. Such tropical cyclones reach Northern Oman once every 5–10 years (Weyhenmeyer et al., 2000, Weyhenmeyer et al., 2002).

Fluvial drainage system along the north-eastern Oman margin is characterized by numerous, small ephemeral streams (wadis) that drain the Oman mountain range (Fig. 2). The rare but intense rainfall usually causes catastrophic flooding ("flash floods") of these systems. The most important fluvial system along the south-eastern Oman margin is the wadi Al Batha that reaches the Gulf of Oman just south of the Ras al Haad (Figs. 1, 2). It is constituted by numerous tributaries that drain the northern edges of the Wahiba desert sands, the Oman Mountains (including the Sama'il ophiolite), and Quaternary alluvial deposits (Garzanti et al., 2003). The Wahiba desert sand develops to

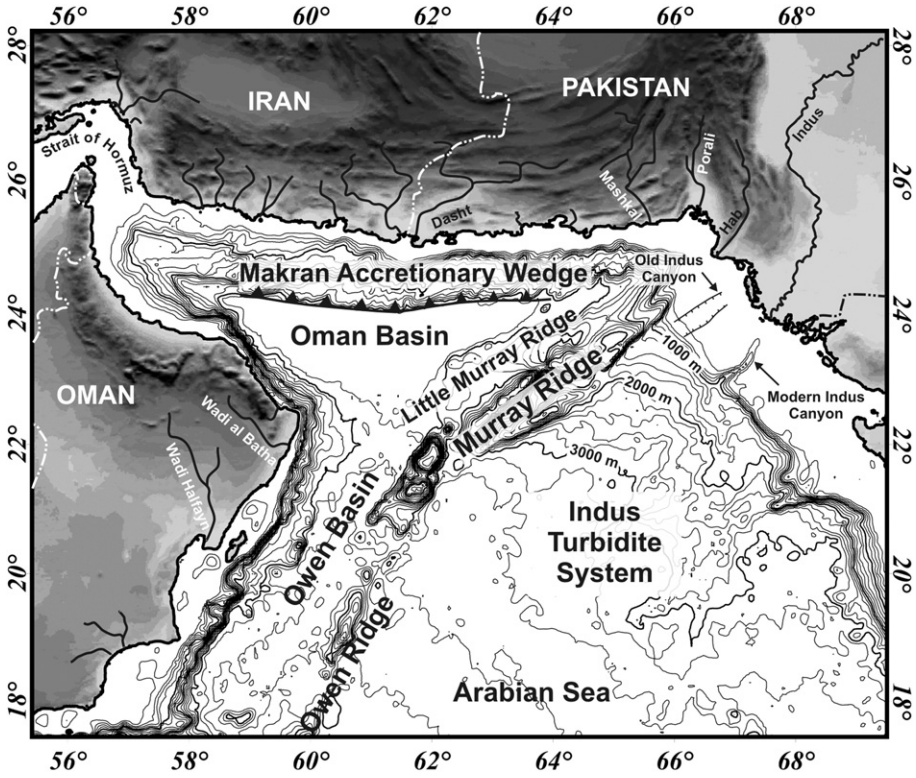

Fig. 1. General map of the Gulf of Oman (Arabian Sea, NW Indian Ocean). Bathymetric contours (in meters) are from the ETOPO 2 database.

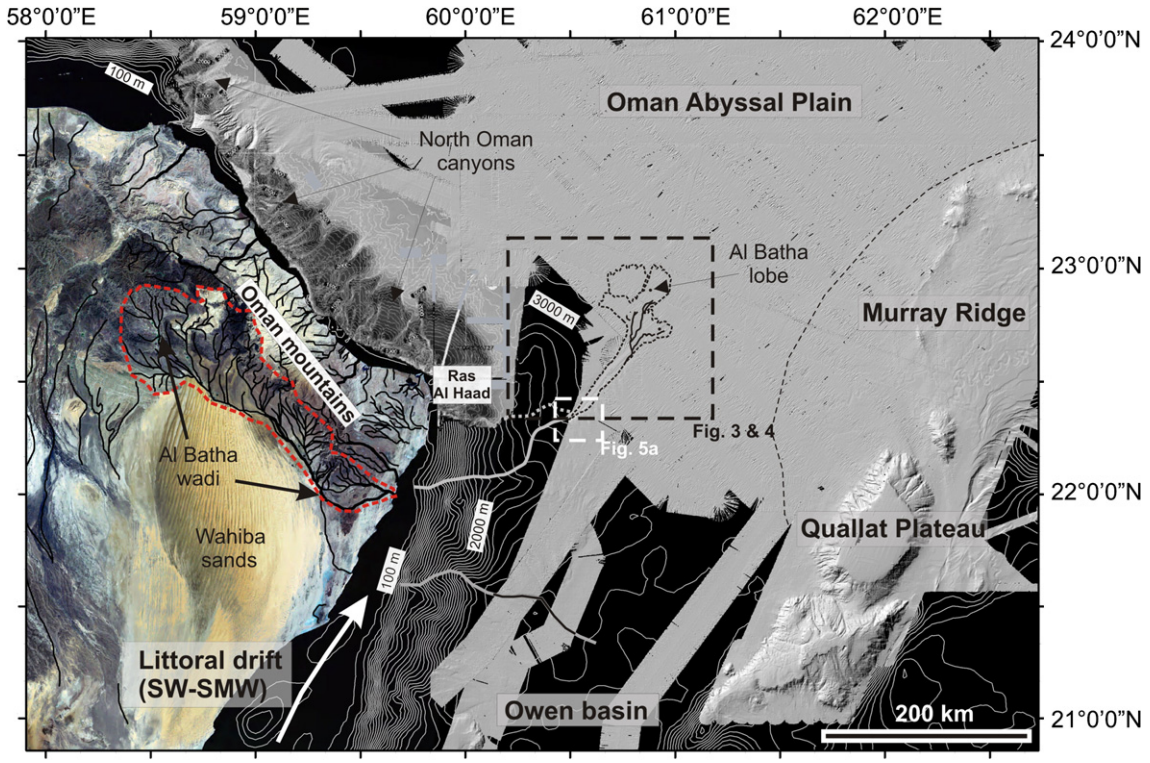

Fig. 2. Physiographic map of the study area showing localization of the main drainage basins and deep-sea sedimentary systems (see location in Fig. 1). Shaded bathymetry of the North-Western area (North Oman canyons) has been redrawn from the data of Szuman et al. (2006). Red dashed line delimitates the Al Batha wadi watershed. The white arrow represents the summer monsoon-induced SW–NE littoral drift along the Oman coast.

the south, with a coastline composed of coastal dune cliffs up to 20 m high (Radies et al., 2004), in an area where the fluvial input is quasi-absent (only the southern branch of the Al Batha wadi (Fig. 2) reaches the Oman coast in this area).

At present, sediment along the south-eastern Oman margin is transported north-eastward, towards the Ras al Haad, in longshore drift until it is likely intercepted by the Al Batha canyon head at the downdrift end of the littoral cell, where the continental shelf significantly narrows (Fig. 2). Additional sediment might be transported through resuspension by storm waves and rip currents, and advected north-eastward by the prevailing current.

3. Materials and methods

3.1. Acoustic and seismic mapping

The bathymetry and acoustic imagery was collected using the multibeam echosounder SIMRAD EM12 and EM300 during the MARABIE 2000 (*R/V Atalante*, IFREMER) and MARABIE 2001 (*R/V Le Suroît*, IFREMER) surveys, respectively. Additional multibeam bathymetry and more than 800 km of sub-bottom seismic lines (SBP 120 profiler) were collected during the FanIndien cruise (*R/V Beautemps-Beaupré*, SHOM), among them 400 km in the Al Batha lobe area (Figs. 3, 4). The SBP 120 sub-bottom profiler offer deeper penetration in the bottom and higher resolution (~1 m) than conventional sub-bottom systems, with sweep frequencies between 2, 5 and 7 kHz. It allows a very detailed observation of the upper 100 m in fine-grained sediments, and ~25 m in sand-rich floor.

3.2. Core data

Two piston cores (Table 1) were collected (using the Kullenberg corer) in the Al Batha lobe during the MARABIE 2001 survey. Thin slabs (15 mm thick) were sampled and analyzed in the SCOPIX X-ray image processing tool (Migeon et al., 1999). Additionally, grain-size analyses were performed using a Malvern™ Supersizer 'S'. Microscopical observations of thin-sections (10 cm long) of impregnated sediments selected from well-preserved sedimentary facies were performed using a fully automated Leica™DM6000B Digital Microscope (Zaragosi et al., 2006). Two AMS ^{14}C dating were done on core KS05 (Table 2), from bulk planktonic foraminifer species sampled in hemipelagic clay intervals.

The top of core KS05 is composed of visually massive sand (~105 cm thick) whereas X-ray imagery shows vertical deformation structures (Fig. 9). Piston coring within coarse material often provides short penetration and coring disturbances, and thus this layer is interpreted as coring artefact. Hence, only the base of core KS05 (55 cm) was analysed.

4. Morphology of the Oman margin and distribution of the sedimentary systems

The Oman margin is characterized by a strong north–south asymmetry (Uchupi et al., 2002; Fig. 2). The cape Ras Al Haad (Fig. 2) separates the northern and southern physiographic provinces.

In the north, the continental shelf is narrow (from 2 to 7 km). The outer shelf is incised by a network of canyons with steep walls, U-shaped cross sections, and relief in excess of 100 m (Uchupi et al., 2002). These canyons are 1–3 km wide in the upper slope, 50–90 km long, and they seem to be directly connected to the network of wadis that reaches the northern Oman coast (Fig. 2). At the toe of slope, small channels occasionally develop but rapidly disappear on the available bathymetry data (Szuman et al., 2006). Downstream of these systems, our data does not show any significant sedimentary bodies in the abyssal plain.

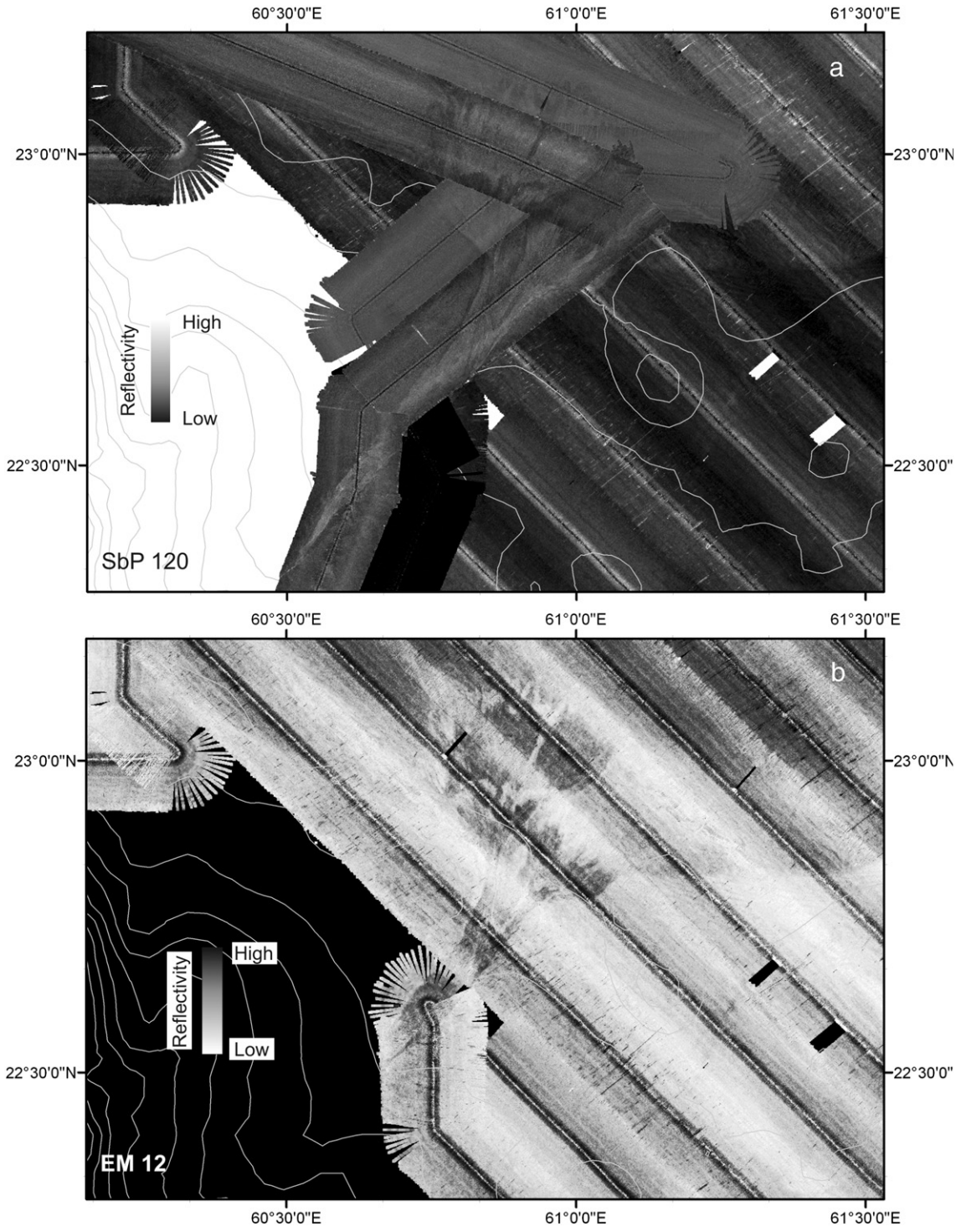

Fig. 3. Acoustic imagery of the Al Batha turbidite lobe and feeder system: a) SbP 120 data collected during the FanIndien cruise. b) EM 12 data. Note that the backscatter intensity scale is inversed on the two pictures.

Southward, in the region of the Ras Al Haad, the continental shelf is less than 10 km wide and extends down to ~110 m water depth (Fig. 2). The upper slope is characterized by steep slope gradients (up to 4°) until the depth of 2200 m. The lower slope shows lower gradients (~0.8°) and reaches the abyssal plain at 3100 m water depth. The latter has low slope gradient (<0.1°) towards the centre of the Oman basin (Fig. 2) that is limited eastward by the Murray ridge (Fig. 2). The main sediment depocenter along the Oman margin is the Al Batha turbidite system that develops south of the Ras Al Haad, forming a lobe that extends in the abyssal plain for over 1000 km^2 (Figs. 2, 3, 4). South of the Al Batha turbidite system, sediment depocenter shift towards the southern Owen basin, that is 150 km wide and confined by the Owen ridge (Fig. 2). The slope is characterized by tilted blocks aligned parallel to the margin's strike (Uchupi et al., 2002). Off the southern branch of the Al Batha wadi, a slope valley develops down to the Owen basin (Figs. 1, 2). Further to the south, the continental shelf widens, and the

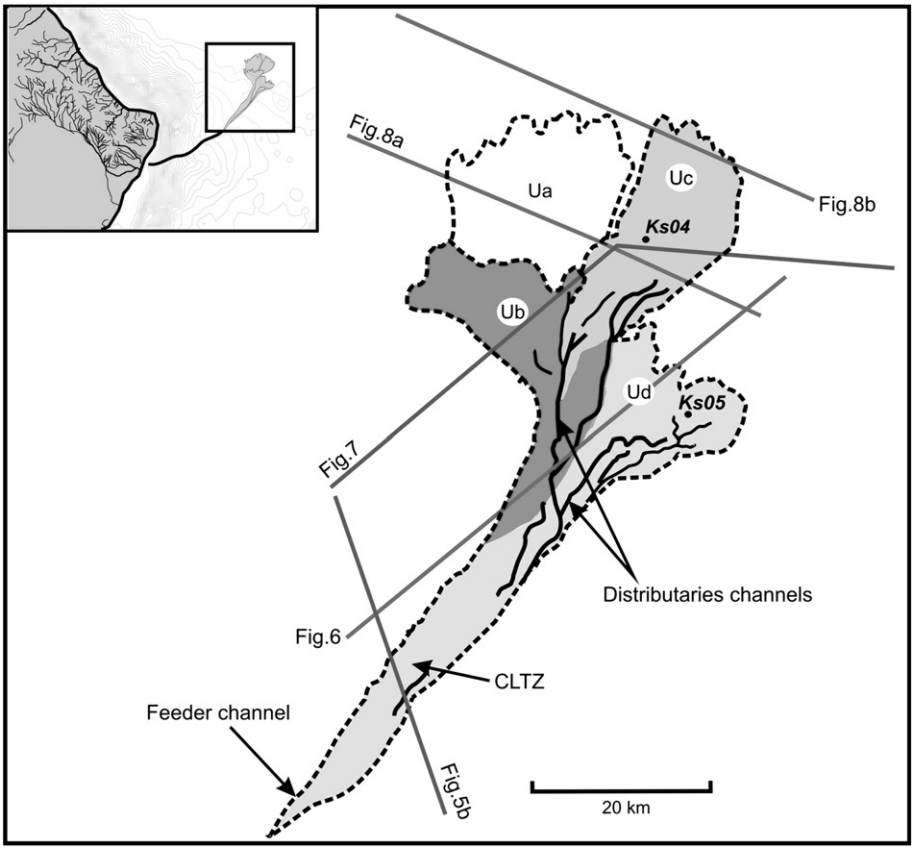

Fig. 4. Interpretative scheme of the Al Batha lobe complex with localization of the sub-bottom seismic lines and sedimentary cores. The four lobe internal units have been named Ua–d (see text for details).

absence of wadis along the southern Oman coast suggests that there is low sediment input into the Owen basin.

5. The Al Batha turbidite system

5.1. Feeder system and channel–lobe connection

The multibeam bathymetry coverage begins at 2900 m water depth (less than 100 km from the present coastline), where the Al Batha channel is 2 km wide (Fig. 5A). There, the right flank of the channel is ~130 m high, whereas its left flank is characterized by a 25 m levee. Downstream, the feeder channel rapidly widens and becomes relatively flat-floored, with small depressions that are poorly resolved on the bathymetry at this scale. At −3070 m, the right flank remains 60 m high, while the left levee is almost absent (Fig. 5A). This strong, persistent asymmetry suggests either that the system developed a very thick right levee as it is observed in the Hueneme turbidite system (Piper et al., 1999), or that the channel course is confined by a structural high on its right side.

On sub-bottom seismic data, the axial area consists of a transparent to chaotic acoustic facies, with very low penetration, suggesting occurrence of coarse deposits (Fig. 5B). Several small scours < 10 m deep and 200–300 m wide are observed. Theses structures are also identified on bathymetry (Fig. 5A), and can be continuous along several kilometres (Fig. 5A). The right flank is composed of high amplitude, continuous bedded reflectors (Fig. 5B). The left, near-flat border is characterized by medium to low amplitude continuous bedded facies. Local slump deposits are also observed at the foot of the right levee (Fig. 5B).

Comparable scoured zones have been described in several recent and ancient turbidite systems and probably represents the channel–lobe transition zone (CLTZ; e.g., Wynn et al., 2002a,b). In the Al Batha turbidite system, the CLTZ extends longitudinally on approximately 25–35 km, until the occurrence of the channelized lobe body (Figs. 4, 5A).

5.2. Morphological elements

The Al Batha lobe complex is ~95 km long (including the channel–lobe transition zone), reaches a maximum of 41 km in width, and has a surface area of about 1030 km^2. Acoustic imagery reveals at least four elongated low reflectivity units (Fig. 3). These units have been named "a" to "d" without any references to their age or order of deposition

Table 1
Location of cores.

Core number	Latitude	Longitude	Depth (m)	Length (m)	Cruise	Year	Institute
KS04	22°59,90′ N	60°57,50′ E	3345	1.25	MARABIE I	2001	SHOM
KS05	22°48,9′ N	61°00,01′ E	3316	1.6	MARABIE I	2001	SHOM

Core number, latitude, longitude, water depth, length and cruise details of investigated cores.

Table 2
AMS 14C age origin.

Core number	Depth (cm)	Uncorrected 14C age BP	Calendar age BP	Species analysed	Origin
KS05	108–111	1250 ± 120	804	Planctonic foraminifers (bulk)	Poznań Radiocarb. Lab. — 6561
KS05	130–133	2900 ± 30	2692	Planctonic foraminifers (bulk)	Poznań Radiocarb. Lab. — 6564

Radiocarbon dates have been corrected for a marine reservoir effect of 408 years and calibrated to calendar years using CALIB Rev 5.0/Marine04 data set (Stuiver and Reimer, 1993; Stuiver et al., 2005).

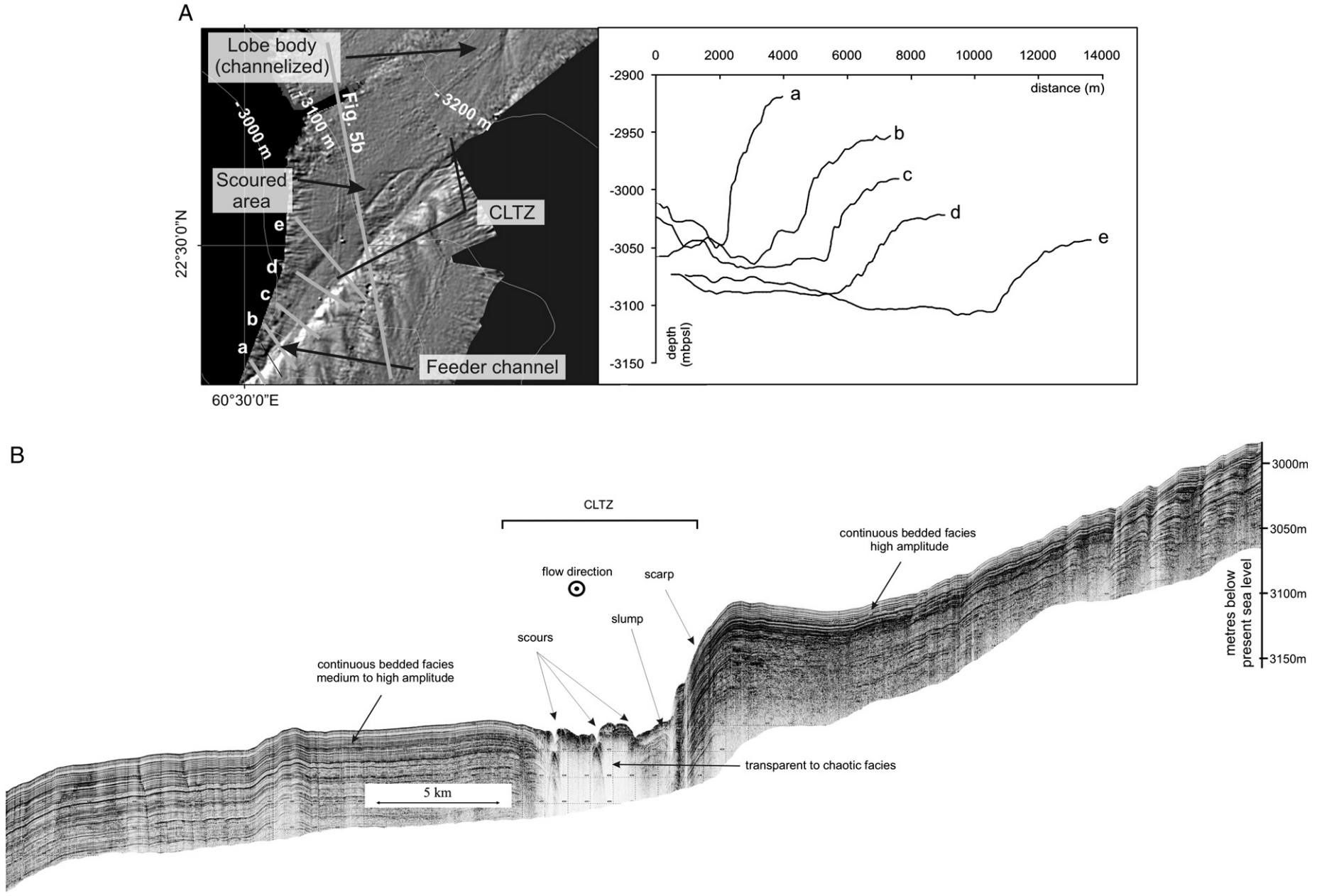

Fig. 5. A: Shaded bathymetry (SbP 120) of the channel–lobe transition zone and transverse bathymetric profiles (a to e). B: Sub-bottom seismic line in the CLTZ illustrating the scoured, low seismic penetration bottom floor and the general asymmetry with a well-developed right levee. Depths are given in meters below present sea level (mbpsl).

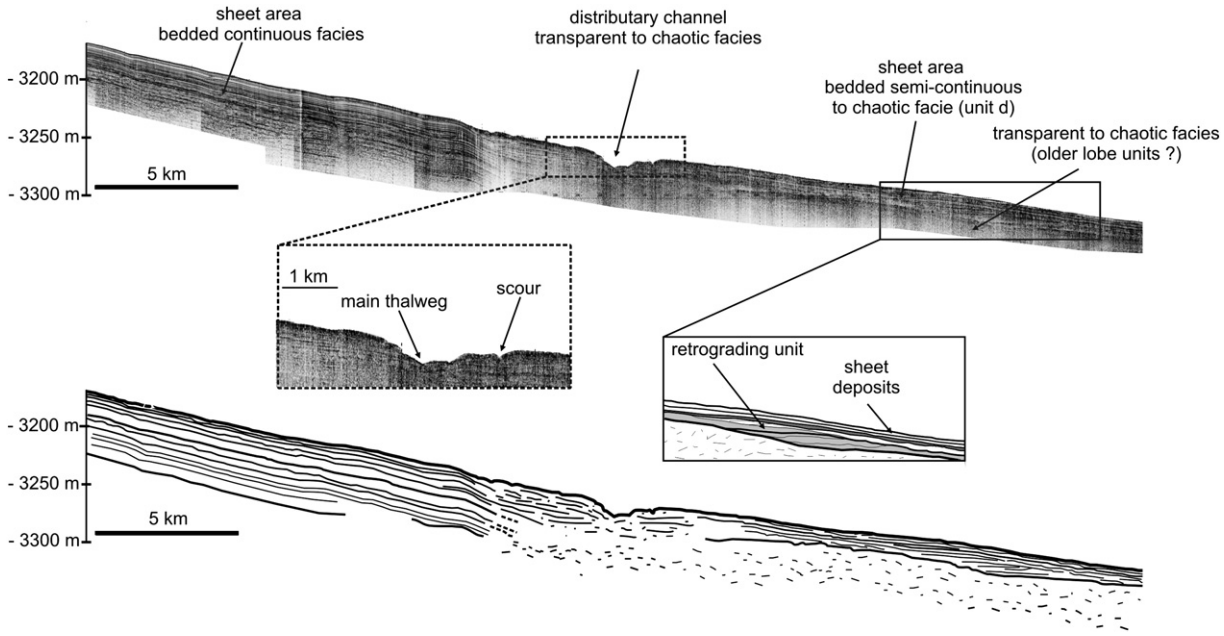

Fig. 6. Sub-bottom seismic line illustrating the general geometry of the proximal lobe with an erosive distributary channel.

(Fig. 4). They are about 10–17 km wide and ~20 km long. Their margins have crenulated edges, and show relatively abrupt transition with the surrounding high-backscattering sea floor. The plan view architecture of these units suggests that they are both laterally and vertically stacked. The proximal lobe is characterized by lineaments of higher reflectivity (Fig. 3), interpreted as small axial feeder channels. These channels rapidly splay into several smaller distributaries (with high backscatters) observed in unit b, c and d (Figs. 3, 4) from several avulsion knickpoints. The size of these channels is difficult to evaluate due to the data resolution, but they are generally less than 1 km wide. Lineaments of higher backscatters are no longer observed in the middle and distal lobe (Fig. 3). A distributary channel (<1 km wide and ~20 m deep) truncating older lobe deposits is observed in the proximal area of lobe unit b (Fig. 6). Laterally, the left flank of the channel shows sheet-like, medium to high amplitude facies, related to either overbank (fine-grained) deposits or hemipelagites. Downlobe, small scours or channel-like features are observed in unit b (Fig. 7) suggesting that erosion, transport, and deposition processes are active in this area.

5.3. Seismic facies and geometries

The Al Batha lobe is characterized by irregular acoustic reflections, where transparent to chaotic facies dominate. Lobe complex thickness is difficult to assess due to the low penetration of the seismic signal, and is estimated to be ~20–30 m on each line (Fig. 7).

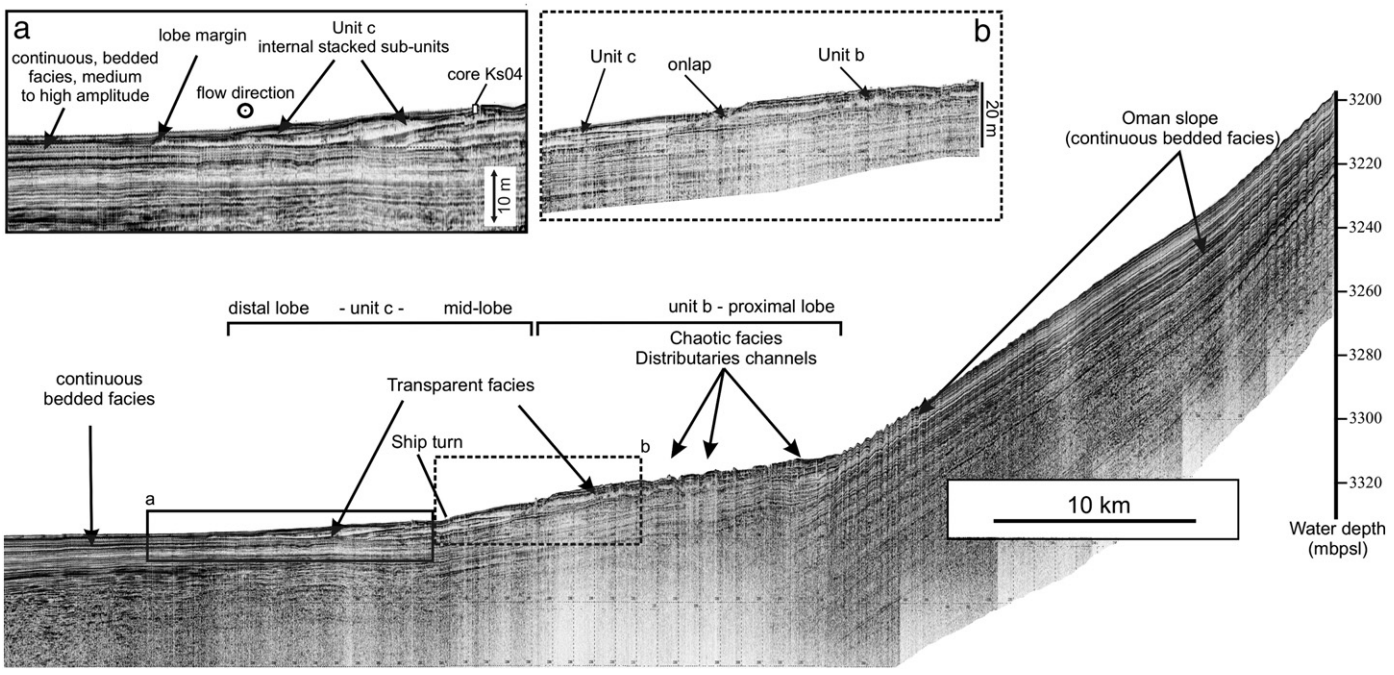

Fig. 7. Sub-bottom seismic line illustrating the transverse and longitudinal geometry within the lobe units b and c.

At the scale of the sub-bottom seismic, the lobe is composed of individual lenses with a transparent to chaotic acoustic facies. These elementary bodies are generally a few metres thick (from 5 to less than 0.5 m) and can be laterally continuous for several kilometres. Thinner lenses are rarely observed due to limitation of seismic data vertical resolution. The lenses are considered as elementary depositional bodies separated by single, high amplitude continuous drape reflectors (Figs. 7, 8, see also Twichell et al., 1992; Gervais et al., 2006b). Continuous to semi-continuous, high to medium amplitude bedded acoustic facies (Figs. 6, 7, 8) is interpreted as overbank deposits (e.g., Piper et al., 1999) or background (hemipelagic/pelagic) sedimentation.

At the scale of elementary bodies, the organization is dominated by the lateral and vertical stacking of individual bodies (i.e. aggradation and lateral migration; Figs. 7, 8a). In the channelized proximal lobe, elementary bodies are generally characterized by a lens-shaped morphology of low lateral extension (generally less than 2 km) and complex stacking (Fig. 7). In the mid-lobe area, channels are no longer observable on either multibeam bathymetry or seismic profiles (Figs. 3, 4, 7, 8a), and the deposits consist of vertically stacked tabular to lens-shaped elementary bodies that are generally less than 5 m thick and can be laterally continuous for several kilometres (in places for more than 10 km; Fig. 8a). This suggests that by-pass decreases downlobe, leading to sheet (tabular) deposition of residual material in the mid-lobe area.

The distal lobe is characterized by isolated acoustically transparent lenses, interbedded with sheet-like deposits, composed of continuous bedded facies of variable reflector amplitudes (Fig. 8b). Isolated lenses are usually 1–2 m thick, with a maximum extension of 500–600 m (Fig. 8b). As observed in proximal areas, these lens-shaped bodies have sharp upper and lower boundaries (high amplitude reflector), and they have an un-stratified, transparent acoustic character.

Longitudinal geometry at the scale of elementary bodies has been only partially observed due to the sparse seismic data. However, we could observe retrograding elementary bodies at some locations, (e.g., unit c in Fig. 7 and unit d in Fig. 6). Such small-scale internal architecture has been observed previously in the south Golo lobe (Gervais et al., 2006b). At the lobe margin (Fig. 7) the elementary bodies pinch-out laterally and/or are onlapped by a sheet-like deposit, characterized by continuous bedded facies.

At the scale of lobe internal units, organization results from the lateral shift of the depocenter. This is illustrated by the onlap geometry between the units c and b (Fig. 7). This is also observed downstream with the simple, lateral stacking of elementary bodies from the units c and a (Fig. 8a). The lateral migration of the internal units is likely linked with avulsions of the main channels in the proximal lobe, as suggested by acoustic imagery (Figs. 3 and 4). However, more data is needed to further characterize the architecture and the timing of deposition of the whole lobe units.

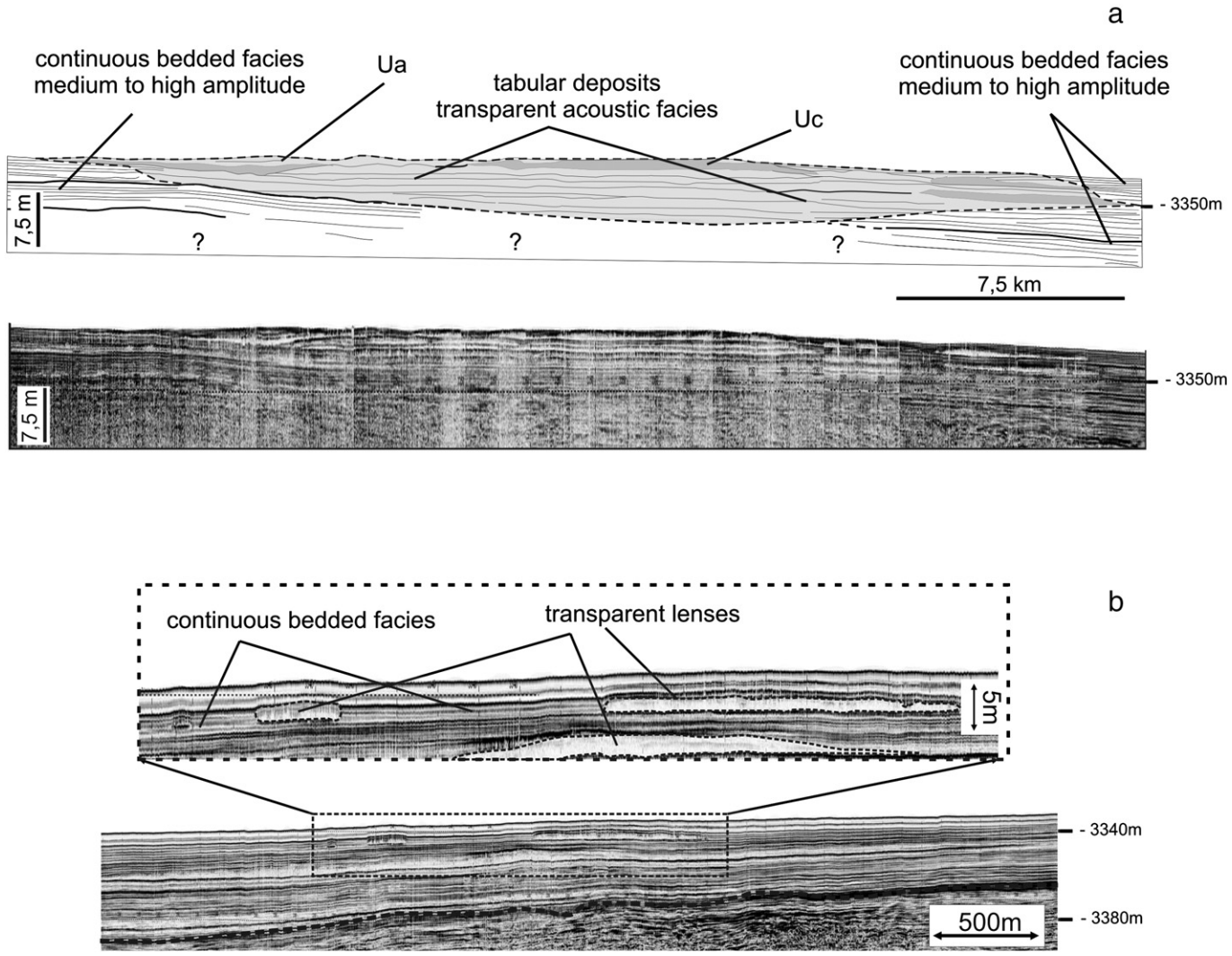

Fig. 8. Sub-bottom seismic lines illustrating the transverse geometry of the mid-lobe and distal fringe.

Table 3
Sedimentary facies description and characteristics.

Facies name	Sedimentological characteristics	Association	Interpretation
Facies I: bioturbated clay	(<5 cm thick): light grey, foraminifer-rich, fine-grained (~5–6 μm), bioturbated clay (Fig. 11). Basal contact is gradual	At the top of Facies IIb and III	Hemipelagite/pelagite
Facies IIa: laminated silty layer	(<5 cm thick): grey–brown silt and silty clay, showing planar laminae, and inversely graded (from ~10 to 70 μm). The basal contact is often gradual, and the upper contact is often erosional (Fig. 11)	At the base of Facies IIb, III, and IV gradual transition above Facies I (Fig. 11)	Deposits of a waxing turbidity flow (e.g. Kneller, 1995; Mulder et al., 2003)
Facies IIb: normally graded sand to silt deposits	(<10 cm thick): brown–grey very fine sand, silt and silty clay, with possible planar lamination, and normally graded (from ~120 to 6 μm). The basal contact is net or slighlty erosional, and the upper contact is often gradual (Fig. 11)	Above Facies I with a sharp or slighlty erosional contact Above facies IIa with a sharp or slightly erosional contact	Td–Te Bouma's division (Bouma, 1962); deposits of a waning turbidity flow (e.g. Piper and Deptuck, 1997)
Facies III: sandy deposits with basal mud clasts	(18–38 cm thick): dark brown to grey sand, massive or slighlty graded (from 194 to 116 μm), structureless. The basal contact is erosional, often with incorporation of silty clast from the underlying sediment (Fig. 10) of small diameter (<2 cm), with irregular edges. A larger, rounded clast is observed (>10 cm) in core KS04 (Fig. 9)	Above Facies I and IIa with a clear erosional contact (Fig. 10) Above Facies IV (sharp or gradual contact)	Deposition from a concentrated flow sensus Mulder and Alexander, 2001 (Ta division of Bouma, 1962)
Facies IV: disorganized sand and silt–clay clasts	(27 cm thick): massive or poorly graded medium to fine sand (~150 μm) showing no sedimentary structure, mixed with abundant (>50%) silt–clay clasts (~8–15 μm) of variable size (max. 10 cm). Clasts have very irregular shape and edges. Towards the top, clasts become thinner (a few mm) and finer (~6 μm) (Fig. 11)	Above Facies IIa with an erosional contact (Fig. 11)	Deposition from a concentrated flow sensus Mulder and Alexander, 2001 (Ta division of Bouma, 1962)

5.4. Sedimentary facies associations

Although only two short piston cores were recovered, they provide useful indications on the sedimentary processes involved in the formation of the Al Batha lobe. Four sedimentary facies were identified in several vertical facies associations. These facies are described in Table 3 and illustrated in Figs. 9–13. Bioturbated, foraminifer-rich clay is assigned to Facies I, and is interpreted as hemipelagic/pelagic deposits. Facies IIa consists of coarsening-upward, silt–mud laminae (from 10 to 70 μm), whereas fining-upward sand to silt (from 120 to ~6 μm) is assigned to Facies IIb. Facies III is characterized by massive or slightly graded sand (from 194 to 116 μm), with possible mud clasts near the base of bed. Finally, massive or poorly graded disorganized sand (~150 μm) with silt–mud clasts (8–15μm) is assigned to Facies IV.

5.4.1. Facies association 1 (Facies I–IIb–I)

Facies association 1 consists of the vertical succession of Facies I (hemipelagite) and Facies IIb (fining-upward sand to silt layer), with a sharp or slightly erosional basal contact and a very gradual top contact. This association is observed in both cores, but is volumetrically more significant in core KS05 (Figs. 9, 12). It is interpreted as the classical vertical stack of turbidite–hemipelagite deposition (e.g., Bouma, 1962).

5.4.2. Facies association 2 (Facies I–IIa–IIb–I)

This association consists of the vertical succession of Facies I (hemipelagite/pelagite) and Facies IIa (coarsening-upward silt–mud laminae) with a gradational basal contact. Facies IIa is capped by Facies IIb (fining-upward sand to silt layer). A slightly erosional surface (Figs. 11, 12) is present between Facies IIa and IIb, which fines up into silty clay, (Bouma Te division) and then into Facies I (hemipelagic sedimentation). This association is observed in core KS04 (115–102 cm; Fig. 9).

5.4.3. Facies association 3a (Facies IIa–III–IIb–I)

This association (Figs. 10, 12) consists of Facies IIa (inversely graded layer) capped by a massive to slightly normally graded sand (Facies III, D50 ~160–150 μm) that fines up into Facies IIb (fining-upward sand to silt layer). An erosional contact is present between Facies IIa and IIb. The facies association is capped with a gradual transition into hemipelagic deposits (Facies I). Within the first few centimetres of Facies III, mm-thick mud clasts with internal planar laminations typically occur. This association is observed in core KS04 (Fig. 10) and at the base of core KS05, where only the top of the sequence is recovered (Fig. 9).

5.4.4. Facies association 3b (I–IIa–IV–III)

This association (Figs. 11, 12) consists of the vertical succession of Facies I (hemipelagite/pelagite), Facies IIa (coarsening-upward silt–mud laminae) and Facies IV (~27 cm thick disorganized fine sand and silt–mud clasts). An erosional surface is present between Facies IIa and IV. At the top, Facies IV grades into a 38 cm thick massive sand layer (Facies III) with a large (>10 cm), rounded mud clast (Fig. 9). This association is only observed in core KS04 (35–67 cm; Fig. 9).

5.5. Sediment composition and sediment source

Turbidite sands (Fig. 10) mainly consist (>40%) of angular to subangular quartz crystals (mono- and polycrystalline) and carbonates that attest of a fluvial transport. The next largest population of grains is composed of rounded carbonate material of aeolian origin (~30%). Rare plagioclases, clinopyroxenes crystals, and rounded serpentinized fragments with cellular textures are observed. This assemblage corresponds to a mixed mineral assemblage from the Wahibah desert sands and Sama'il ophiolitic belt, both drained by the wadi Al Batha (Garzanti et al., 2003). Micrite grains and shell fragments (mollusks) are also observed, as well as mixed benthic and planktonic foraminifera tests (~20%), probably incorporated along the gravity flows path.

5.6. Interpretations of the facies associations

Facies association 1 consists of thin fine sand to silt layers (with few planar laminations) that grade upward into mud (Figs. 9, 10, 12). This association is here interpreted as single depositional event from the uppermost and diluted part of a turbulent flow that spills over turbidite-channel levees (Hesse and Chough, 1980; Piper and Deptuck, 1997). In the case of lobe depositional environment, thin-bedded fine-grained turbidites (KS05; Fig. 9) can be interpreted as a result of sheet deposition from the diluted and turbulent tail and/ or cloud of concentrated flows that can easily spill over small distributary channels (Gervais et al., 2006a).

Facies associations 2, 3a and 3b are composed by a thin, inversely graded basal layer (Facies IIa). Facies IIa shows grain-size increase of several tens of micrometers (see Figs. 10 and 11). Several processes can produce inversely graded facies. One of them is the incorporation of mud clasts at the base of structureless turbidite layers. These clasts

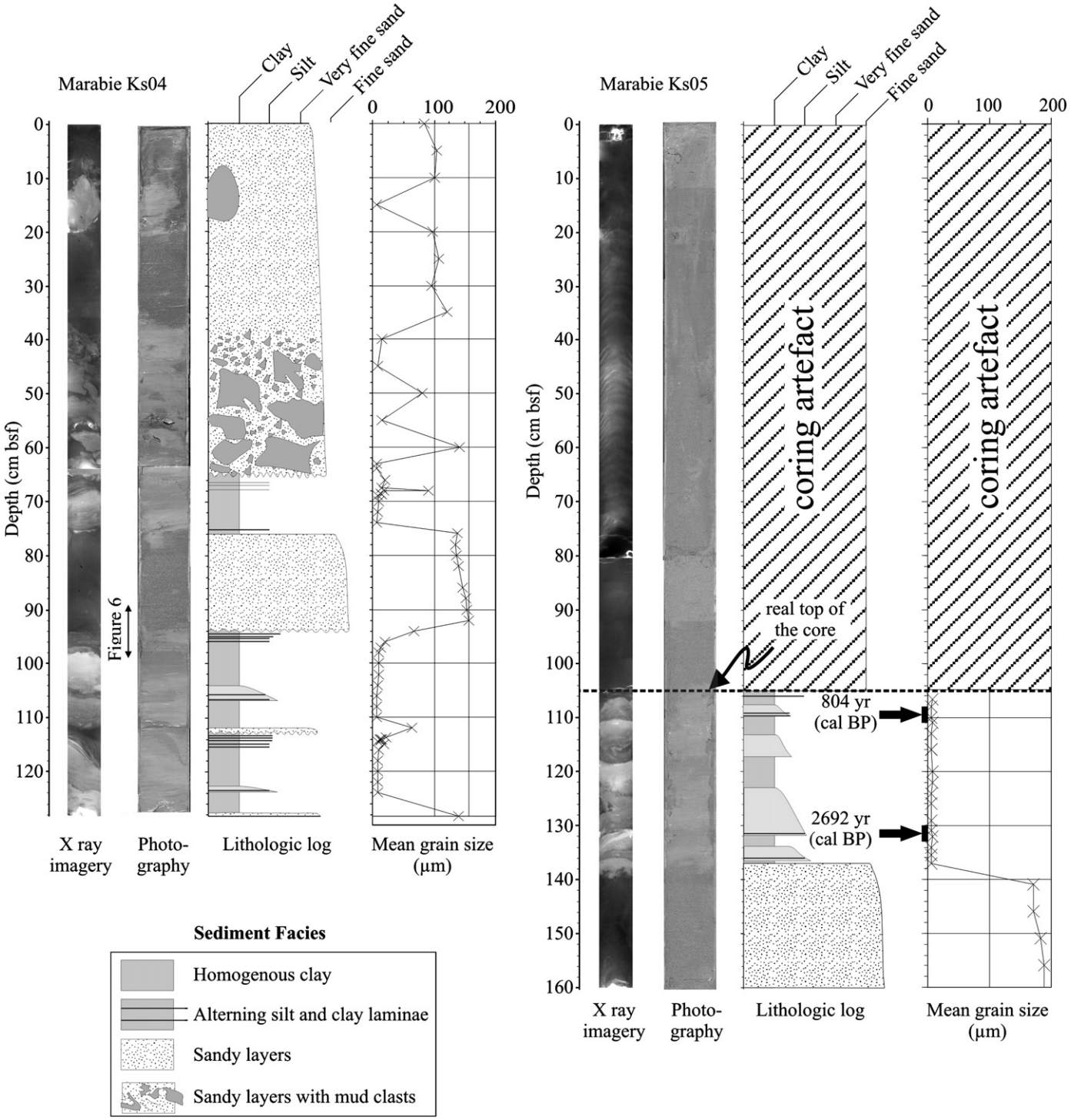

Fig. 9. Photography, X-rays and detailed lithologic log of the sedimentary cores KS04 and KS05, with grain-size analysis and position of the two AMS 14C dating.

contribute to a local decrease of the mean grain size, and may result in a sampling artefact by generating millimetre- to centimeter-thick inverse grading (Mulder et al., 2001). However, mud clasts are never observed within Facies IIa (neither visually nor on X-ray images), Furthermore, Facies IIa commonly show planar lamination, and its basal contact is always gradual, suggesting a low degree or lack of erosion. Inversely graded layers may also develop under highly concentrated basal part of gravity currents (see Mulder and Alexander, 2001). Such layers result from the deposition by freezing of a coarse-grained (gravel or coarse sand), massive layer in a concentrated or hyperconcentrated gravity flow (e.g., R2 unit of the Lowe sequence; Lowe, 1982). However, Facies IIa consists of thin silt–mud laminae (see Table 3 and Figs. 10, 11) and thus can not corresponds to Lowe sequences.

Thus, the inversely graded basal layer is interpreted to result from the deposition by a waxing (accelerating with time), depletive flow (Kneller, 1995; Kneller and Buckee, 2000; Mulder and Alexander, 2001), which can deposit a coarsening-up unit as long as the flow velocity is below the erosion threshold (Kneller, 1995). Facies IIa is found capped by a fining-upward layer, resulting of the deposition by

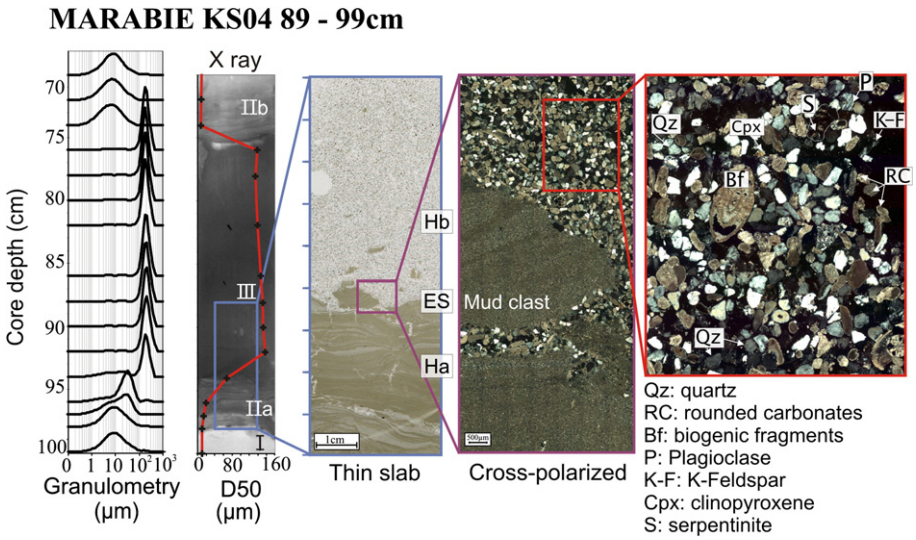

Fig. 10. X-ray, grain-size analysis and thin slab showing the facies association 3a (core KS04). Close-up views show the main petrologic assemblages of the turbidite sands.

a waning (decelerating with time) concentrated or turbulent flow (Bouma, 1962; Kneller, 1995; Mulder and Alexander, 2001 and references therein). Mulder et al. (2001) interpreted such bed architecture as a result of a flood-generated turbidity current (suspended-load dominated hyperpycnal flow). The resulting deposit ("hyperpycnite") consists of a basal coarsening-upward layer deposited during the waxing period at the river mouth (Ha), and a fining-upward layer (Hb) related to the waning period of the flood discharge. These two

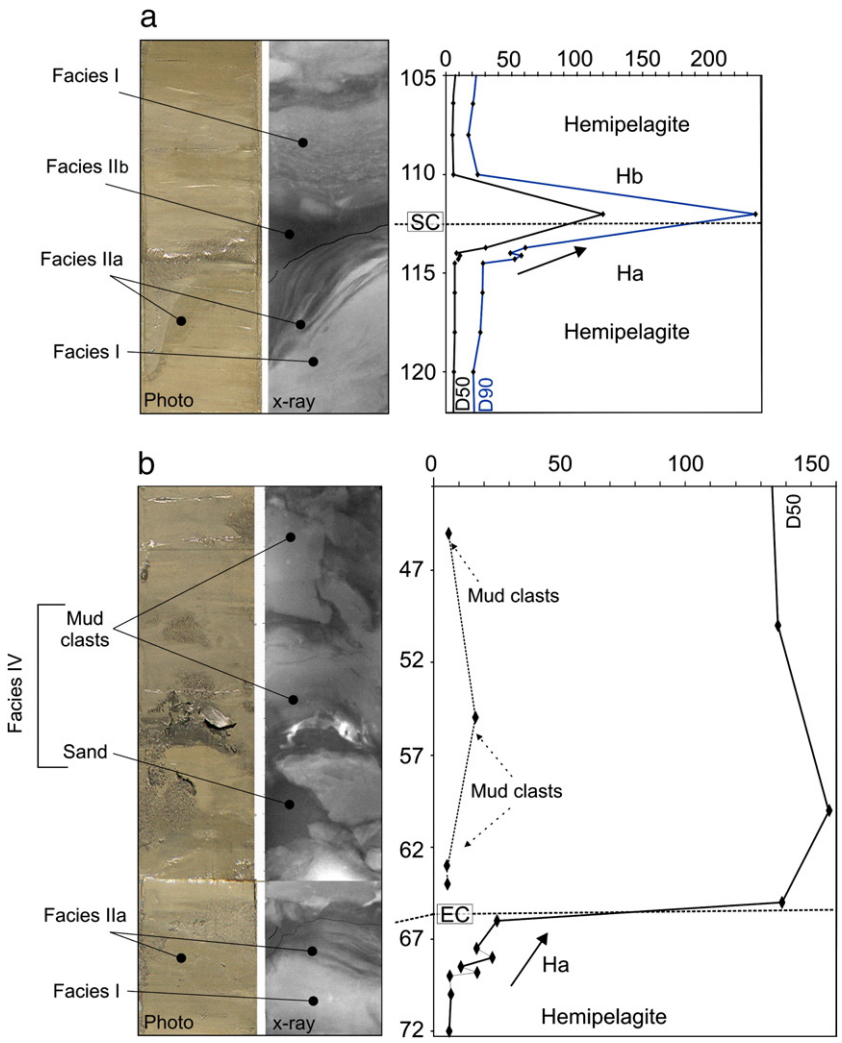

Fig. 11. Photography, X-ray and grain-size analysis showing the facies association 2 (fine-grained hyperpycnite) and 3b (sand, mud-clasts-rich hyperpycnite).

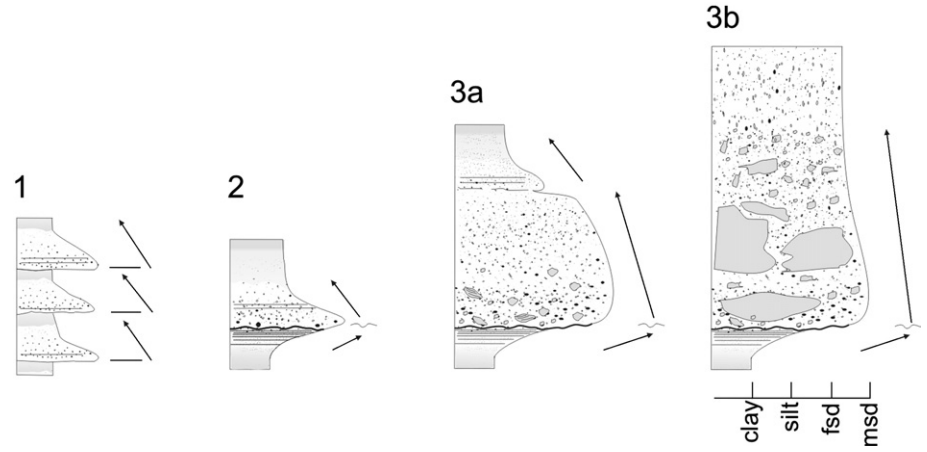

Fig. 12. Synthetic logs of the four facies association observed in the Al Batha lobe (refer to text for detailed description).

stacked layers are classically separated by an erosional intrabed contact (attributed to maximum erosion, Figs. 10, 11), which corresponds approximately to the peak river flood, i.e. maximum suspended load discharged by the river (Mulder et al., 2003; Plink-Björklund and Steel, 2004).

Alternatively, reverse-to-normally graded layers, separated by an internal erosion surface, have been also observed locally at the base of ancient large volume, basin wide turbidite beds (e.g., Talling et al., 2007), interpreted as slope failure-generated turbidites. In that case, the turbidite beds were too voluminous to be generated by flood discharge in the ocean, and the authors proposed that the internal bed architecture was more likely produced by waxing and waning turbidity currents produced by single or repeated landslides (Talling et al., 2007). Such deposits are related to rare, unchannelized, large volume turbidity currents that create thick sheet deposits continuous on hundreds of kilometres (Wynn et al., 2002a,b; Talling et al., 2007). Inversely, the Facies Associations 2, 3a and 3b described in the Al Batha lobe form only centimetre to decimetre-thick beds of low lateral extension (i.e. confined lobe deposits), related to channelled turbidity flows of moderate volume. In addition, the low regional seismicity associated to the regional physiographic context (that allows a low residence time of the sediments on the shelf and a rapid transfer in the Al Batha canyon) suggest that mass wasting is not the dominant processes in the area. This is also suggested by the absence of slump or debris flow deposits in both coring and seismic data, as well as by the mineralogy of the turbidite sands that indicates a continental origin. The presence of coal fragments and leaves in the turbidite beds is an usual criterion to discriminate gravity deposits originated from river flood (Mulder et al., 2003; Plink-Björklund and Steel, 2004; Nakajima, 2006; Zavala et al., 2006). Although turbidite sands of the Al Batha lobe are devoid of continental organic matter, this criterion is not valid in the Oman margin setting, as the wadi Batha drainage basin is an arid region with almost no vegetation cover. Finally, we interpret the facies associations 2, 3a and 3b as a result of waxing and waning flows related to Al Batha wadi floods.

Thus, Facies association 2 is interpreted as a fine-grained hyperpycnite: the Ha unit consists of coarsening-upward mud laminae deposited by combined traction and fallout in a waxing flow (Mulder and Alexander, 2001). In facies association 2a, Ha is capped by a fining-upward silty layer that grades into mud. This normal grading suggests deposition by a waning turbulent flow (Figs. 11, 12). It roughly corresponds to the hyperpycnite-type deposits of Mulder et al. (2003).

Facies association 3a is interpreted as a sandy hyperpycnite (Figs. 10, 12). The Ha layer is ~4 cm thick, and is interpreted similarly to facies association 2. It is capped by a massive or poorly graded sand layer that grades upward into a thin fining-upward turbidite through a

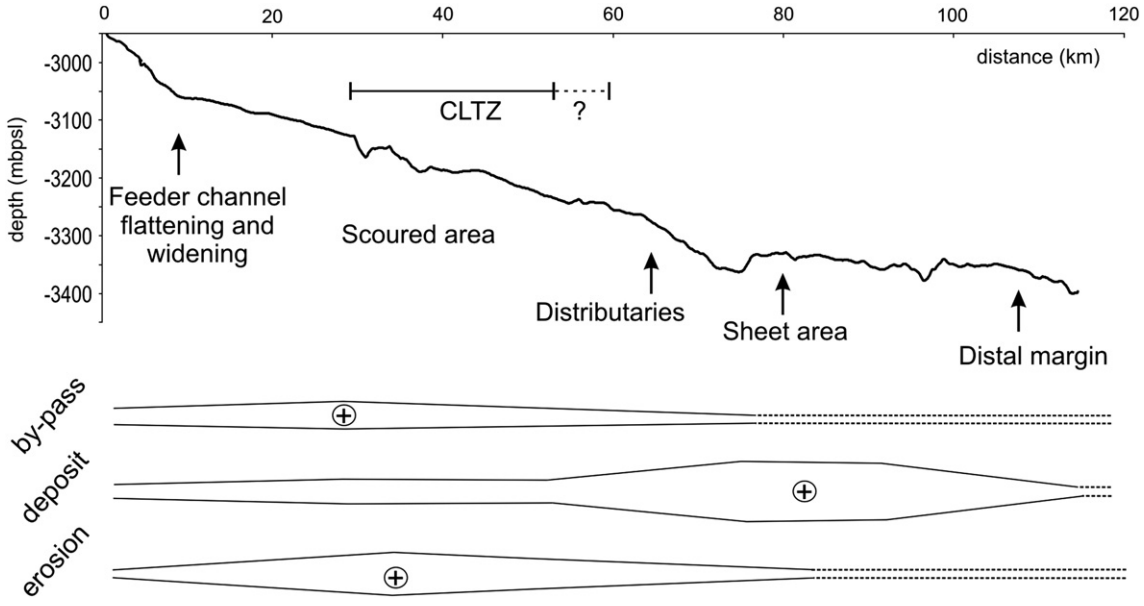

Fig. 13. Simplified longitudinal organisation of the Al Batha lobe and evolution of by-pass, deposition, and erosion processes along the slope gradient.

by-pass surface (resulting in a break of grain size). Such deposits are commonly interpreted as the result of the initial rapid fallout of the coarse material (Bouma, 1962) transported in the thin concentrated layer at the bottom of the flow (Mulder and Alexander, 2001). It is capped by a thin deposit from the turbidity flow tail and/or cloud (Td and Te divisions separated from Ta by a sharp contact; Figs. 10, 12). This facies association illustrates the vertical concentration gradient in a bipartite gravity flow (Mulder and Alexander, 2001; Mutti et al., 2003).

Facies association 3b is similar to facies association 3a, but the high proportion of large floating mud clasts within a thicker massive sand layer (Facies IV, Hb) suggest the existence of upward dispersive pressure associated with buoyant lift (Lowe, 1982) as reported by Gervais et al. (2006a) in the Golo lobe deposits. Facies association 3b is thus related to deposition by a more concentrated, laminar flow (Mulder and Alexander, 2001). Mud clasts in Facies IV show grain sizes that range between 5 and 10 μm (i.e. clay to silty clay). Clasts thin-upward (Figs. 11, 12) and generally have sharp edges, suggesting little erosion within the sand-rich flow, and thus a short transport.

5.7. Vertical trends in cores

The core KS05 is mainly composed of Facies association 1, whereas the core KS04 is dominated by thick sandy deposits (FA 2, 3a and 3b; Fig. 9).Two AMS-datings have been obtained from bulk planktonic foraminifera in the hemipelagic beds (Facies I) at the base of two turbidites in the core KS05 (Fig. 9). They provide ages of cal 804 and 2692 years before present, showing that the Al Batha turbidite system has been active recently (i.e. during the present sea-level highstand).

6. Discussion

6.1. Lobe architecture

The Al Batha lobe is composed of at least four sub-surface units, fed by a diverging network of small distributary channels. Our data suggests that the lobe complex is not directly connected to the feeder (channel–levee) system. In our study, the resolution of the bathymetry and acoustic imagery prevent a fine characterization of the transition zone (CLTZ). However, we identified the presence of erosional features (scours) associated with a very poor acoustic penetration characteristic of coarse-grained deposits (Fig. 5B). Channel–lobe transition zones are generally dominated by erosion and by-pass, with sparse sand deposition, and are though to provide a good sand connectivity (Wynn et al., 2002a,b). CLTZ is frequently observed in recent turbidite systems, and their formation may depend on the size and efficiency of the feeder systems (i.e. the composition, volume and frequency of the flows) as well as the basin morphology and sea floor sediment composition (Wynn et al., 2002a,b).

In the Al Batha lobe, the scours seem to merge downcurrent and form small channels (Figs. 4, 5a). These channels rapidly splay into smaller distributaries that fed the lobe units (Fig. 4), suggesting rapid migration of the flows pathway through small avulsion of the lobe channels. Small avulsions (i.e. channel branching) in the proximal and mid-lobe areas is also suggested by the incorporation of mud clasts in much of the sandy deposits, usually concentrated near the base of the beds. This is also a common feature of sandy lobes deposits (e.g., Nelson et al., 1992; Kenyon et al., 2002; Klaucke et al., 2004; Bonnel, 2005; Gervais et al., 2006a). Indeed, in proximal and mid-lobe areas, concentrated flows (or the basal parts of bipartite gravity flows) that remain confined in the small distributaries, move across the lobe and can easily erode older overbank deposits at the channel margins (see Gervais et al., 2006b). This can lead to rapid deposition of the over-concentrated basal part of the flows whereas a significant part of the material is carried out downlobe and remain confined to the end of the channel until flow collapse. This small-scale migration is typical of lobe architecture (Normark et al., 1979; Twichell et al., 1992; Piper et al., 1999; Zaragosi et al., 2000; Zaragosi et al., 2001; Klaucke et al., 2004; Gervais et al., 2006b) and is fundamental for the understanding of the lobe morphology, as it is responsible for the occurrence of the highly discontinuous channel, channel mouth, and channel margins deposits interfingering within the lobe (Twichell et al., 1992; Gervais et al., 2006b). The migration thus primarily controls the sand body connectivity.

In the Al Batha lobe, the distributary channels progressively disappear downlobe, suggesting that by-pass and erosional processes decrease while successively more deposition takes place. At the mouth of these small channels, the slope gradient decreases (Fig. 13), leading to the decrease of the flow competence, and the deposition of sheet, tabular or lens-shaped sand-rich deposits (Figs. 8a, 13). The mid-lobe area thus corresponds to the area of preferential deposition in the basin (Normark, 1978).

The distal lobe (lobe fringe) consists of a few, isolated transparent lenses stacked within drape-like, thin-bedded sediments (Fig. 8b). These small lenses (1–2 m thick with less than 600 m extent) probably represent the final, sandy deposition from the most energetic flows, stacked into the fine-grained sediments, i.e. fine-grained turbidites and/or hemipelagites (Fig. 8b).

The general organization of the lobe (Fig. 13) is similar to what has been described from the basin plain lobes of East Corsica margin (Gervais et al., 2006b; Deptuck et al., 2008) and the Hueneme fan (Piper et al., 1999): a channelized proximal lobe, where by-pass, erosion, and deposition coexist; a depositional mid-lobe area of tabular sands with better homogeneity; and the distal lobe fringe, dominated by sheet-like fine-grained deposits with a few residual sand lenses.

6.2. Compensation stacking

The architecture of the elementary bodies that compose the Al Batha lobe have a similar topographic compensational architecture as proposed by Mutti and Sonnino (1981), resulting in a simple vertical (aggradation) and lateral (migration) stacking of the lobe deposits. Deptuck et al. (2008) recognized several levels of compensational stacking that control the lobe architecture at various spatial and temporal scales. Because of low slope gradients, topographic compensation is probably a key mechanism for deposition in lobe environments, and thus the degree of confinement of the flows (i.e. the pre-existing topography) will predominantly determine the three-dimensional geometry of the lobe (Gervais et al., 2006b). In the proximal areas, flows are channelled and confined between the older deposits, and deposition occurs in topographic lows (Fig. 7). In the mid-lobe (Fig. 8a), the deposits are mainly tabular, with a good lateral continuity. They are vertically stacked by topographic compensation, and the lateral migration is less frequent than in the proximal lobe. This may be explained by a weaker confinement of the flows in this area, as they rapidly lost their capacity at the mouth of the small distributaries (Normark and Piper, 1991; Mulder and Alexander, 2001). Such mid-lobe architecture is often described in sand-rich lobes as the Hueneme, Var, and Golo lobes (Piper et al., 1999; Bonnel, 2005; Gervais et al., 2006b).

At a larger scale, the planar-view architecture of the four lobe units suggests that they are both laterally and vertically stacked (Fig. 3, 4), and therefore it is likely that they have been built by a combination of repeated major avulsions of the main distributaries in the proximal part (i.e. lateral shift), and retrogradation/progradation of the lobe units during their growth, as observed for the Var and Golo lobes (e.g., Bonnel, 2005; Gervais et al., 2006b).

6.3. Flow initiation

From our data, and regarding to the physiographic context, we suggest that several types of processes can lead to the initiation of gravity flows in the Al Batha turbidite system. As the head of the Al

Batha canyon cut the narrow Oman shelf (Fig. 2), it is likely influenced by both coastal hydrodynamic processes and river input, in particular during sea-level lowstand conditions. Seismicity in the area is not significant and is likely to be negligible in comparison to other triggering mechanisms.

Storm waves and rip-current erosion of sediment from the canyon head can induce small failures of poorly consolidated littoral sands accumulated near the canyon head by the SW–NE littoral drift, and generate sand-rich gravity flows (Gaudin et al., 2006). Such mud-poor flows are generally inefficient and therefore, deposit sand rapidly (Piper et al., 1999), and would probably not significantly contribute to the distal lobe development. Rip-current erosion of sediment from the canyon head may have also contributed to gravity flow initiation during sea-level lowstand conditions, but the canyon head is at present localized too far from the coastline, out of the rip-current and storm wave influence zone. Alternatively, our sedimentological data suggest that flood-related gravity flows have contributed to the development to the Al Batha turbidite system, at least during sea-level lowstand conditions, allowing a direct connection between the wadi Al Batha and the canyon head. Ephemeral, high-gradient streams located in an arid environment have a high efficiency to carry bulk sediment and deliver large amounts of material during occasional and catastrophic flooding (Milliman and Syvitski, 1992; Laronne and Reid, 1993), and the Al Batha wadi can be qualified to 'dirty river' (following Milliman and Syvitski, 1992) highly susceptible to produce hyperpycnal flows at recurrence times of years (Mulder and Syvitski, 1995; Mulder et al., 2003).

Observation of complete hyperpycnites in distal deposits is suspected to be rare since the waning part of the flow (related to the peak flood) tend to overtake distally the slower-moving, waxing part of the flow, so that in the most downstream locations it is likely that there is no inverse-graded layer (Mulder and Alexander, 2001; Kneller and McCaffrey, 2003). Furthermore, most of the Oman wadis floods are intense and of short duration (i.e. flash floods) in response to heavy rainfalls of a few hours (generally less than 20 h). Although such short but intense events carry significant amounts of suspended material to the coast, and are likely to transform into hyperpycnal currents upon arrival in the marine basin (Mulder et al., 2003), it is more likely that insignificant deposition occurs in areas were the flows are waxing, as their initial velocity increases quickly and deposits are rapidly eroded (Mulder and Alexander, 2001). Alternatively, rare but heavy thunderstorms can cause intensive rainfall and flooding of the Oman wadis for several days (Fuchs and Buerkert, 2008), as what was observed during the recent Gonu cyclone (June 2007). Thus, only extreme events that generate sustained, high-concentration underflows are likely recorded in the Al Batha lobe, hence increasing time of waxing discharge that in turn can be recorded at some locations in the distal deposits. Holocene fine-grained hyperpycnites of the Toyama turbidite system lobes are suggested to have a recurrence time of 70 years (Nakajima, 2006), indicating that only a few extreme flood events would deposit in such distal area (at least during highstands).

Finally, several types of gravity flows, with different triggering mechanisms and grain-size characteristics, may have contributed to the development of the Al Batha turbidite system, but more data is needed to investigate the evolution of sedimentary processes through times.

6.4. Characteristics of the hyperpycnal flow beds

Within the Facies Association 3a, and 3b, the important drop in grain size associated with the erosional contact between Ha and Hb (Fig. 12) is related to flow transformation after the peak discharge (cf. Mulder et al., 2003 and Zavala et al., 2006) and evolution of concentrations within a sustained, flood-generated gravity flow. The basal layer is interpreted to be deposited by a waxing, low-concentration turbulent flow, and partially eroded by a co-genetic, basal concentrated bipartite flow (Fig. 12). The important change in grain size and the presence of the intrabed erosional surface can result from the high-concentrated river load during the peak discharge conditions (cf. Prior and Bornhold, 1989). Furthermore, the sandy hyperpycnites observed in the Al Batha lobe are similar to the "dam"-breaking hyperpycnites described by Mulder et al. (2003), with "a top missing hyperpycnite in the beginning of the flood, capped by either a mass-flow or a hyperconcentrated flow deposit, and a base missing hyperpycnite resulting from the end of the flood". They interpret this facies association as the result of failure of a natural dam due to the flood. It corresponds to extreme events, with a higher flow concentration and a greater run-out potential than in flood-related, suspended-load dominated hyperpycnal flow (Mulder et al., 1998; Zuffa et al., 2000; Nakajima, 2006).

This mechanism may be an analogous to the erosion and entrainment of the mouth-bars sediments at the peak flood that is likely to occur in the wave-dominated setting of the wadi Batha mouth. Indeed, the fluvial input of the wadi Al Batha is low or even missing and the accretion of littoral-drift sediments at the stream mouth by the wave and tidal action forms huge sand bars. In addition, enhanced erosion in the stream bed is classically observed in ephemeral, gravely-bed streams in arid and semi-arid environments, and is typical of Oman wadis, where the availability of coarse sediments is intensified by the lack of vegetation cover (Laronne and Reid, 1993; Fuchs and Buerkert, 2008). Intense flooding of desert streams can generate subaerial hyperconcentrated flows (Batalla et al., 1999), that can transform into subaqueous, high-concentration underflows at the stream mouth (Mutti et al., 1996; Mulder et al., 2003). These mechanisms could generate a critical and rapid increase in sediment concentration at the peak of the flood, and enhanced sand transport towards the marine basin.

6.5. Relations between basin setting and lobe shape and architecture

The parameters that control lobe depositional characteristics have been studied for a long time as the lobes are considered as an important reservoir potential for hydrocarbon (Galloway, 1998). Most of the principal concepts come from outcrop studies (e.g., Mutti and Normark, 1991). Galloway (1998) proposed that grain size is an important parameter leading to the formation of "mounded", coarse-grained lobes, with channelization in the proximal lobe, and "sheet" lobes composed of finer sediments, consisting of low-relief, channelized bodies with more heterogeneity. Recently, insights provided by outcrop-scale seismic data in modern environment showed that this concept overlooks crucial parameters such as the initial confinement of the depositional environment (see Gervais et al., 2006b) as well as the changes in the frequency of sediment supply in response to climato-eustatic variations (e.g., Piper et al., 1999; Deptuck et al., 2008). However, the characteristics of sediment input and the initiation mechanisms for turbidity currents are the most important variables that influence the shape of turbidite systems because they directly influence the style of individual elements and subelements (Reading and Richards, 1994; Piper and Normark, 2001).

The example of the Oman margin provides new evidences on the parameters controlling the architecture of the turbidite systems. The size of the drainage basin, the margin morphology and the sand distribution within the Oman basin have several similarities with the East and West Corsica systems (Kenyon et al., 2002; Gervais et al., 2006a). Several morphologic features described in the Al Batha lobe are also similar to those described in the Golo, Hueneme, Var, and probably Navy turbidite lobes (cf. Normark et al., 1979; Piper et al., 1999; Bonnel, 2005; Gervais et al., 2006b; Deptuck et al., 2008). These lobes generally have a rounded morphology. They also have a similar longitudinal organization with, from proximal to distal: (1) an area of by-pass and erosion, with shallow channels; (2) an area of sheet sand

deposition corresponding to the mid-lobe and (3) an area of fine-grained deposition corresponding to the lobe margins and fringe (Fig. 13). All the turbidites systems listed above correspond to relatively small, sand/mud rich systems fed by small mountainous (dirty) rivers (*sensu* Milliman and Syvitski, 1992). Inversely, lobes in large river-fed turbidite systems that develop along low gradient, passive margins (such as the Mississippi or Zaire lobes) show a more elongated morphology and are highly channelized (Twichell et al., 1991; Savoye et al., 2000; Bonnel, 2005). The same observations are made for the basin plain lobes of the Nile turbidite system (Migeon et al., 2010-this volume). High efficiency, thick turbulent flows that occur in large, "mud rich" turbidite systems (e.g., Zaire, Mississippi or Nile systems) build highly ramified elongated lobes, in which more various deposits are stacked, including long run-out debrites and fine-grained and sandy flows deposits (Nelson et al., 1992; Migeon et al., 2010-this volume). Lobes associated with smaller sandy systems are heterogeneous (at least at some locations), but have the potential to have a better sand connectivity (Reading and Richards, 1994; Galloway, 1998).

6.6. Architecture of the margin with respect to turbidite reservoir models

Although the Oman margin is at present times considered as a passive margin (Uchupi et al., 2002), the southern margin has been a zone of active deformation, probably margin-parallel shear (Barton et al., 1990). This is illustrated by the margin N–S dissymmetry that involves two different basin settings, separated by the Ras Al Haad (Fig. 2).

The north-eastern Oman margin can be considered as a typical submarine ramp (following Reading and Richards, 1994), characterized by multiple canyons–channels that develop along steep to moderate slope gradients (Fig. 2). Numerous wadis deliver sediments from the Oman mountains coastal range and reach the Gulf of Oman (Fig. 2). A close relationship has been observed between the wadis mouth and the location of canyon heads at the shelf break (Szuman et al., 2006). As they are typical high-gradient ephemeral streams, it is likely that the wadis can deliver sediments directly in canyon heads (at least during sea-level lowstands).

The southern Oman margin, marked by a shift of the depocenter towards the Owen basin (Fig. 2), is characterized by tectonic-induced more complex slope morphology, illustrated by the presence of small ridges and through parallel to the margin, such as the Masirah ridge (Barton et al., 1990). Fluvial input is restricted to the southernmost branch of the wadi Al Batha that seem to feed a submarine valley that finally reaches the confined Owen basin (Fig. 2). The Wahiba desert sand extends southward, and sediments can only be transported on the larger continental shelf by the monsoonal littoral drift (Fig. 2). Despite the poor available data, we believe that the southern margin is probably characterized by low sediment input, a few channelized systems, and is likely to be considered as a slope apron in a confined setting.

The Al Batha turbidite system develops at the boundary of these two physiographic areas, and can be considered as sand–mud rich, point source submarine fan (Reading and Richards, 1994), although we do not have precise information on the proximal part of the system (canyon, channel–levee). The unusual size of the Al Batha system in the Oman basin (regarding to the whole margin) is related to a combination of (i) its connection with the major fluvial input from the Oman landmass, and minor contribution from a smaller wadi-connected canyon (Fig. 2); (ii) the narrowing of the continental shelf (that disappears south of the Ras Al Haad, Fig. 2) associated with the monsoon-related drift that can carry sediments down to the canyon head. At a regional scale, the Al Batha turbidite system can thus be defined as a sediment trap. Although many similarities appear between the margin architecture of the western and eastern Corsica systems (Kenyon et al., 2002; Gervais et al., 2004), our results indicate that the Al Batha turbidite system remains active at present time (Fig. 9), whereas both western and eastern Corsica systems are inactive during highstands. The Al Batha turbidite system could be an analogous to the highstand active California borderlands turbidite systems (Piper et al., 1999; Covault et al., 2007), located in a quite similar setting (e.g., where hyperpycnal flows significantly contributed to the systems growth and where the longshore drift-transported sediment also contributes to the canyon heads where the shelf narrows significantly).

7. Conclusion

The Oman margin is composed by mid-size turbidite systems strongly influenced by the climatic and geomorphic setting. It is composed of two physiographic provinces: a turbidite system ramp, with small slope valleys connected to multiple small fluvial inputs, compose the north margin; a tectonic-shaped slope apron, with low sediment input and a few channelized systems that fed the confined Owen basin, compose the south margin.

At the boundary between these two provinces, the Al Batha turbidite system is the largest sedimentary accumulation along the Oman margin, and probably acts as a sediment trap. It is a sand and mud rich, point sourced system active during the present day highstand conditions. In the basin plain, it constitutes a ~1000 km^2 sandy lobe that consists of at least four internal units, connected to the feeder channel by a channel–lobe transition zone. Each lobe units consist of several elementary bodies, related to deposition of a single flow. The morphological organization of the Al Batha lobe is similar to a classical architecture model of sand-rich lobes.

Al Batha lobe deposits consist of sandy hyperpycnites, interbedded with fine-grained deposits (turbidites, hyperpycnites or hemipelagites). Although storm waves and rip-current erosion of the littoral-drift sediments accumulated near the Al Batha canyon head may have contributed to the development of the Al Batha turbidite system, the occurrence of sandy hyperpycnites 180 km from the river mouth suggests that the Al Batha turbidite system is directly influenced by catastrophic flooding of the wadi Al Batha.

Acknowledgments

The authors are grateful to the SHOM for making its data available. We are indebted to all scientists, technicians and crew members of the R/V Le Suroît, R/V Atalante and R/V Beautemps-Beaupré for their technical assistance during the Marabie and FanIndien cruises. The authors are also grateful to J. St Paul, B. Martin and G. Chabaud for their technical assistance for core sampling. Finally, we gratefully acknowledge Jérôme Bonnin and W. Fletcher for the English revision, and we benefited from detailed and constructive reviews by Piret Plink-Björklund and co-editor Chris Fielding, that greatly improved the final version of the manuscript.

Julien Bourget PhD thesis is funded by a DGA (French Ministry of Defence)–CNRS doctoral fellowship. This is a UMR CNRS 5805 EPOC (University Bordeaux 1) contribution n. 1689.

References

Barton, P.J., Owen, T.R.E., White, R.S., 1990. The deep structure of the east Oman continental margin: preliminary results and interpretation. Tectonophysics 173, 319–331.
Batalla, R.J., De Jong, C., Ergenzinger, P., Sala, M., 1999. Field observations on hyperconcentrated flows in mountain torrents. Earth Surf. Process. Landf. 24, 247–253.
Bates, C.C., 1953. Rational theory of delta formation. AAPG Bull. 37, 2119–2162.
Bonnel, C., 2005. Mise en place des lobes distaux dans les systèmes turbiditiques actuels: Analyse comparée des systèmes du Zaïre,Var et Rhône. Doctoral Thesis, Talence, Université Bordeaux 1. pp. 314.
Bouma, A.H., 1962. Sedimentology of Some Flysch Deposits: A Graphic Approach to Facies Interpretation. Elsevier, Amsterdam, p. 168.
Byrne, D.E., Sykes, L.R., Davis, D.M., 1992. Great thrust earthquakes and aseismic slip along the plate boundary of the Makran subduction zone. J. Geophys. Res. 97, 449–478.
Clemens, S.C., Prell, W.L., 2003. A 350,000 year summer-monsoon multi-proxy stack from the Owen Ridge, Northern Arabian Sea. Mar. Geol. 201, 35–51.

Covault, J.A., Normark, W.R., Romans, B.W., Graham, S.A., 2007. Highstand fans in the California borderland: the overlooked deep-water depositional systems. Geology 35, 783–786.
Deptuck, M.E., Piper, D.J.W., Savoye, B., Gervais, A., 2008. Dimensions and architecture of late Pleistocene submarine lobes off the northern margin of East Corsica. Sedimentology 55, 869–898.
Ellouz-Zimmermann, N., Lallemant, S., Castilla, R., Mouchot, N., Leturmy, P., Battani, A., Buret, C., Cherel, L., Desaubliaux, G., Deville, E., Ferrand, J., Lügcke, A., Mahieux, G., Mascle, G., Mühr, P., Pierson-Wickmann, A., Robion, P., Schmitz, J., Danish, M., Hasany, S., Shahzad, A., Tabreez, A., 2007. In: Lacombe, O., Lavé, J., Roure, F., Verges, J. (Eds.), Offshore Frontal Part of the Makran Accretionary Prism: The Chamak Survey (Pakistan), pp. 351–366.
Fleitmann, D., Burns, S.J., Mangini, A., Mudelsee, M., Kramers, J., Villa, I., Neff, U., Al-Subbary, A.A., Buettner, A., Hippler, D., Matter, A., 2007. Holocene ITCZ and Indian monsoon dynamics recorded in stalagmites from Oman and Yemen (Socotra). Quat. Sci. Rev. 26, 170–188.
Fournier, M., Patriat, P., Leroy, S., 2008. In situ evidence for dextral active motion at the Arabia–India plate boundary. Nat. Geosci. 1, 54–58.
Fuchs, M., Buerkert, A., 2008. A 20 ka sediment record from the Hajar Mountain range in N-Oman, and its implication for detecting arid–humid periods on the southeastern Arabian Peninsula. Earth Planet. Sci. Lett. 265, 546–558.
Galloway, W.E., 1998. Siliciclastic slope and base-of-slope depositional systems: component facies, stratigraphic architecture, and classification. AAPG Bull. 82, 569–595.
Garzanti, E., Ando, S., Vezzoli, G., Dell'era, D., 2003. From rifted margins to foreland basins: investigating provenance and sediment dispersal across desert Arabia (Oman, U.A.E.). J. Sediment. Res. 73, 572–588.
Gaudin, M., Mulder, T., Cirac, P., Berné, S., Imbert, P., 2006. Past and present sedimentary activity in the Capbreton Canyon, southern Bay of Biscay. Geo-Mar. Lett. 26, 331–345.
Gervais, A., Savoye, B., Piper, D.J.W., Mulder, T., Cremer, M., Pichevin, L., 2004. Present morphology and depositional architecture of a sandy confined submarine system: the Golo turbidite system (eastern margin of Corsica). Geol. Soc. London, Spec. Publ., vol. 222, pp. 59–89.
Gervais, A., Mulder, T., Savoye, B., 2006a. Sediment distribution and evolution of sedimentary processes on the Golo turbidite system (east Corsica, Mediterranean). In: Mulder, T. (Ed.), Special Issue on Deep-Sea Turbidite Systems on French Margins. Geo-Mar. Lett., vol. 26, pp. 373–396.
Gervais, A., Savoye, B., Mulder, T., Gonthier, E., 2006b. Sandy modern turbidite lobes: a new insight from high resolution seismic data. Mar. Pet. Geol. 23, 485–502.
Gordon, R.G., Demets, C., 1989. Present-day motion along the Owen fracture zone and Dalrymple trough in the Arabian Sea. J. Geophys. Res. 94, 5560–5570.
Hesse, R., Chough, S.K., 1980. The Northwest Atlantic Mid-Ocean Channel of the Labrador Sea: II. Deposition of parallel laminated levee-muds from the viscous sublayer of low density turbidity currents. Sedimentology 27, 697–711.
Kenyon, N.H., Klaucke, I., Millington, J., Ivanov, M.K., 2002. Sandy submarine canyon-mouth lobes on the western margin of Corsica and Sardinia, Mediterranean Sea. Mar. Geol. 184, 69–84.
Klaucke, I., Masson, D.G., Kenyon, N.H., Gardner, J.V., 2004. Sedimentary processes of the lower Monterey Fan channel and channel-mouth lobe. Mar. Geol. 206, 181–198.
Kneller, B., Buckee, C., 2000. The structure and fluid mechanics of turbidity currents: a review of some recent studies and their geological implications. Sedimentology. 47 Supplement 1, 62–94.
Kneller, B.C., 1995. Beyond the turbidite paradigm: physical models for deposition of turbidites and their implications for reservoir prediction. In: Hartley, A.J., Prosser, D.J. (Eds.), Characterization of Deep Marine Clastic Systems. Geol. Soc. London, Spec. Publ., pp. 31–49.
Kneller, B.C., McCaffrey, W.D., 2003. The interpretation of vertical sequences in turbidite beds: the influence of longitudinal flow structure. J. Sediment. Res. 73, 706–713.
Laronne, J.B., Reid, I., 1993. Very high rates of bedload sediment transport by ephemeral desert rivers. Nature 366, 148–150.
Lowe, D.R., 1982. Sediment gravity flows: II. Depositional models with special reference to the deposits of high-density turbidity currents. J. Sediment. Petrol. 52, 279–297.
Migeon, S., Ducassou, E., Le Gonidec, Y., Rouillard, P., Mascle, J., Revel-Rolland, M., 2010. Lobe construction and sand/mud segregation by turbidity currents and debris flows on the Western Nile deep-sea fan (Eastern Mediterranean). Sedimentary Geology 229, 124–143 (this volume).
Migeon, S., Weber, O., Faugères, J.C., Saint-Paul, J., 1999. SCOPIX: a new imaging system for core analysis. Geo-Mar. Lett. 18, 251–255.
Milliman, J.D., Syvitski, J.P.M., 1992. Geomorphic/tectonic control of sediment discharge to the ocean: the importance of small mountainous rivers. J. Geol. 100, 525–544.
Mulder, T., Syvitski, J.P.M., 1995. Turbidity currents generated at river mouths during exceptional discharges to the world oceans. J. Geol. 103, 285–299.
Mulder, T., Alexander, J., 2001. The physical character of subaqueous sedimentary density flow and their deposits. Sedimentology 48, 269–299.
Mulder, T., Syvitski, J.P.M., Skene, K.I., 1998. Modeling of erosion and deposition by turbidity currents generated by river mouths. J. Sediment. Res. 68, 124–137.
Mulder, T., Migeon, S., Savoye, B., Faugères, J.C., 2001. Inversely graded turbidite sequences in the deep Mediterranean: a record of deposits from flood-generated turbidity currents? Geo-Mar. Lett. 21, 86–93.
Mulder, T., Syvitski, J.P.M., Migeon, S., Faugeres, J.-C., Savoye, B., 2003. Marine hyperpycnal flows: initiation, behavior and related deposits. A review. Mar. Pet. Geol. 20, 861–882.
Mutti, E., Sonnino, M., 1981. Compensation cycles: a diagnostic feature of turbidite sandstone Lobes. Abstracts Volume IAS 2nd European Regional Meeting 1981, Bologna, pp. 120–123.
Mutti, E., Normark, W.R., 1991. An integrated approach to the study of turbidite systems. In: Weimer, P., Link, M.H. (Eds.), Seismic Facies and Sedimentary Processes of Submarine Fans and Turbidite Systems. Springer-Verlag, New York, pp. 75–106.
Mutti, E., Davoli, G., Tinterri, R., Zavala, C., 1996. The importance of ancient fluvio–deltaic systems dominated by catastrophic flooding in tectonically active basins. Sci. Geol., Mem. 48, 233–291.
Mutti, E., Tinterri, R., Benevelli, G., Biase, D.d., Cavanna, G., 2003. Deltaic, mixed and turbidite sedimentation of ancient foreland basins. Mar. Pet. Geol. 20, 733–755.
Nakajima, T., 2006. Hyperpycnites deposited 700 km away from river mouths in the Central Japan Sea. J. Sediment. Res. 76, 60–73.
Nelson, C.H., Twichell, D.C., Schwab, W.C., Lee, H.J., Kenyon, N.H., 1992. Upper Pleistocene turbidite sand beds and chaotic silt beds in the channelized, distal, outer-fan lobes of the Mississippi fan. Geology 20, 693–696.
Normark, W.R., 1978. Fan valleys, channels, and depositional lobes on modern submarine fans; characters for recognition of sandy turbidite environments. AAPG Bull. 62, 912–931.
Normark, W.R., Piper, D.J.W., 1991. Initiation processes and flow evolution of turbidity currents: implications for the depositional record. Society for Sedimentary Geology. Shorline to Abyss, pp. 207–230.
Normark, W.R., Piper, D.J.W., Hess, G.R., 1979. Distributary channels, sand lobes, and mesotopography of Navy submarine fan, California Borderland, with applications to ancient fan sediments. Sedimentology 26, 749–774.
Piper, D.J.W., Deptuck, M., 1997. Fine-grained turbidites of the Amazon Fan: facies characterization and interpretation. In: Flood, R.D., Piper, D.J.W., Klaus, A., Peterson, L.C. (Eds.), Proceeding of the Ocean Drilling Program, Scientific Results, pp. 79–108.
Piper, D.J.W., Normark, W.R., 2001. Sandy fans—from Amazon to Hueneme and beyond. AAPG Bull. 85, 1407–1438.
Piper, D.J.W., Hiscott, R.N., Normark, W.R., 1999. Outcrop-scale acoustic facies analysis and latest Quaternary development of Hueneme and Dume submarine fans, offshore California. Sedimentology 46, 47–78.
Plink-Björklund, P., Steel, R.J., 2004. Initiation of turbidity currents: outcrop evidence for Eocene hyperpycnal flow turbidites. Sediment. Geol. 165, 29–52.
Prior, D.B., Bornhold, B.D., 1989. Submarine sedimentation on a developing Holocene fan delta. Sedimentology 36, 1053–1076.
Radies, D., Preusser, F., Matter, A., Mange, M., 2004. Eustatic and climatic controls on the development of the Wahiba Sand Sea, Sultanate of Oman. Sedimentology 51, 1359–1385.
Reading, H.G., Richards, M., 1994. Turbidite systems in deep-water basin margins classified by grain size and feeder system. AAPG Bull. 78, 792–822.
Savoye, B., et al., 2000. Structure and recent evolution of the Zaire deep-sea fan: preliminary results of the ZaiAngo 1 and 2 cruises (Angola–Congo margin). Comptes Rendus de l'Academie des Sciences–Series IIA–Earth Planet. Sci., vol. 331, pp. 211–220.
Stuiver, M., Reimer, P.J., 1993. Extended 14C data base and revised CALIB radiocarbon calibration program. Radiocarbon 35, 215–230.
Stuiver, M., Reimer, P.J., Reimer, R.W., 2005. CALIB 5.0. program and documentation.
Szuman, M., Berndt, C., Jacobs, C., Best, A., 2006. Seabed characterization through a range of high-resolution acoustic systems — a case study offshore Oman. Mar. Geophys. Res. 27, 167–180.
Talling, P.J., Amy, L.A., Wynn, R.B., 2007. New insights into the evolution of large-volume turbidity currents: comparison of turbidite shape and previous modelling results. Sedimentology 54, 737–769.
Twichell, D.C., Kenyon, N.H., Parson, L.M., McGregor, B.A., 1991. Depositional patterns of the Mississippi Fan surface: evidence from GLORIA II and high-resolution seismic profiles. In: Weimer, P., Link, M.H. (Eds.), Seismic Facies and Sedimentary Processes of Submarine Fans. Springer-Verlag, New York, pp. 349–363.
Twichell, D.C., Schwab, W.C., Nelson, H.C., Kenyon, N.H., Lee, H.J., 1992. Characteristics of a sandy depositional lobe on the outer Mississippi fan from SeaMARC IA sidescan sonar images. Geology 20, 689–692.
Uchupi, E., Swift, S.A., Ross, D.A., 2002. Morphology and Late Quaternary sedimentation in the Gulf of Oman Basin. Mar. Geophys. Res. 23, 185–208.
Weyhenmeyer, C.E., et al., 2000. Cool glacial temperatures and changes in moisture source recorded in Oman groundwaters. Science. 287, 842–845.
Weyhenmeyer, C.E., Burns, S.J., Waber, H.N., Macumber, P.G., Matter, A., 2002. Isotope study of moisture sources, recharge areas, and groundwater flow paths within the eastern Batinah coastal plain, Sultanate of Oman. Water Resour. Res. 38, 1184.
Wheater, H.S., Bell, N.C., 1983. Northern Oman flood study. Proc. Instn Civ. Engrs, Part 2., vol. 75, pp. 453–473.
Wynn, R.B., Kenyon, N.H., Masson, D.G., Stow, D.A.V., Weaver, P.P.E., 2002a. Characterization and recognition of deep-water channel–lobe transition zones. AAPG Bull. 86, 1441–1462.
Wynn, R.B., Weaver, P.P.E., Masson, D.G., Stow, D.A.V., 2002b. Turbidite depositional architecture across three interconnected deep-water basins on the north-west African margin. Sedimentology 49, 669–695.
Zaragosi, S., Auffret, G.A., Faugères, J.C., Garlan, T., Pujol, C., Cortijo, E., 2000. Physiography and recent sediment distribution of the Celtic Deep-sea Fan, Bay of Biscay. Mar. Geol. 169, 207–237.
Zaragosi, S., Bourillet, J.F., Eynaud, F., Toucanne, S., Denhard, B., Van Toert, A., Lanfumey, V., 2006. The impact of the last European deglaciation on the deep-sea turbidite systems of the Celtic–Armorican margin (Bay of Biscay). Geo-Mar. Lett. 26, 317–329.
Zaragosi, S., Le Suave, R., Bourillet, J.-F., Auffret, G.A., Faugeres, J.-C., Pujol, C., Garlan, T., 2001. The deep-sea Armorican depositional system (Bay of Biscay), a multiple source, ramp model. Geo-Mar. Lett. 20, 219–232.
Zavala, C., Ponce, J.J., Arcuri, M., Drittanti, D., Freije, H., Asensio, M., 2006. Ancient lacustrine hyperpycnites: a depositional model from a case study in the Rayoso Formation (Cretaceous) of West–Central Argentina. J. Sediment. Res. 76, 41–59.
Zuffa, G.G., Normark, W.R., Serra, F., Brunner, C.A., 2000. Turbidite megabeds in an oceanic rift valley recording joekulhlaups of Late Pleistocene glacial lakes of the western United States. J. Geol. 108, 253–274.